CHALMERS

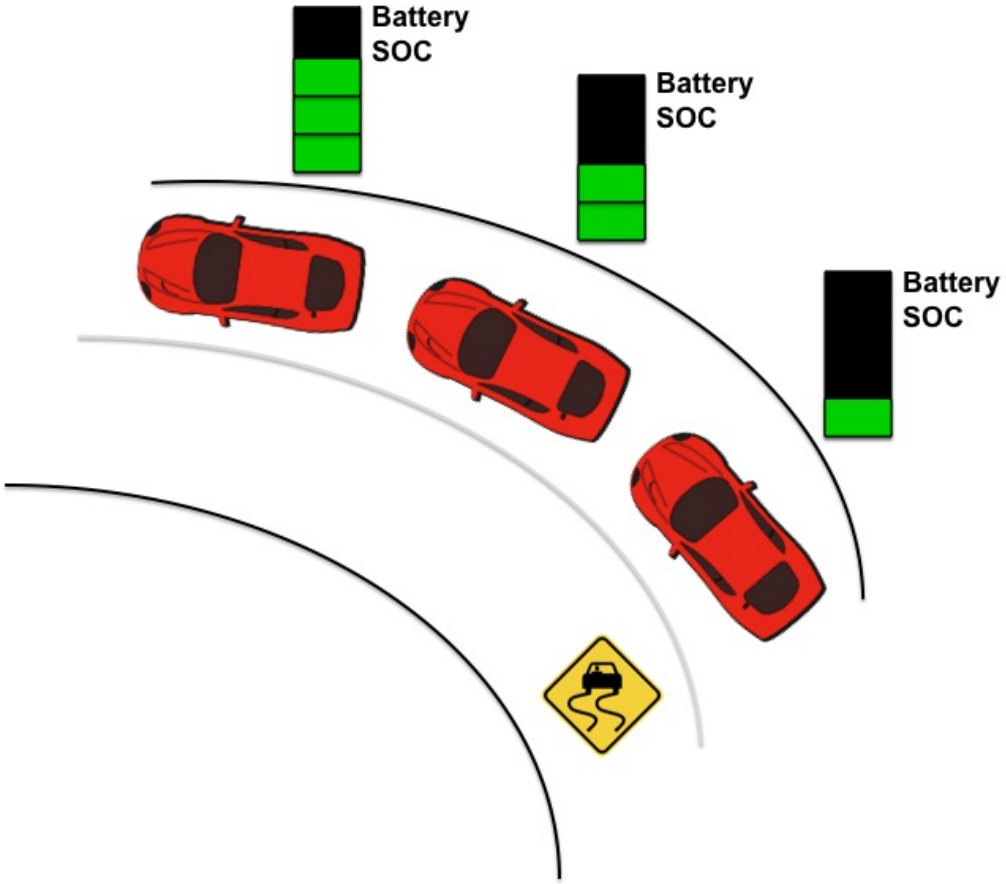

Integrated Vehicle Dynamics Control for Energy Recuperation in Fully Electric Vehicles

Master's Thesis in Systems, Control and Mechatronics

JÓNA MARÍN ÓLAFSDÓTTIR

Department of Signals and Systems
Division of Automatic Control, Automation and Mechatronics
CHALMERS UNIVERSITY OF TECHNOLOGY
Göteborg, Sweden 2011
Master's Thesis EX093/2011

MASTER'S THESIS EX093/2011

Integrated Vehicle Dynamics Control for Energy Recuperation in Fully Electric Vehicles

Master's Thesis in Systems, Control and Mechatronics

JÓNA MARÍN ÓLAFSDÓTTIR

Department of Signals and Systems
Division of Automatic Control, Automation and Mechatronics
CHALMERS UNIVERSITY OF TECHNOLOGY
Göteborg, Sweden 2011

Integrated Vehicle Dynamics Control for Energy Recuperation in Fully Electric Vehicles
JÓNA MARÍN ÓLAFSDÓTTIR

Master's Thesis EX093/2011
Department of Signals and Systems
Division of Automatic Control, Automation and Mechatronics
Chalmers University of Technology
SE-412 96 Göteborg
Sweden
Telephone: + 46 (0)31-772 1000

Chalmers Reproservice
Göteborg, Sweden 2011

Integrated Vehicle Dynamics Control for Energy Recuperation in Fully Electric Vehicles
Master's Thesis in Systems, Control and Mechatronics
JÓNA MARÍN ÓLAFSDÓTTIR
Department of Signals and Systems
Division of Automatic Control, Automation and Mechatronics
Chalmers University of Technology

Abstract

In most fully electric vehicles a regenerative braking system is exploited to extend the vehicle's driving range. With the electric motor generally present at the front axle, delivering the demanded braking solely through regenerative braking can impose stability issues on the vehicle. This is particularly true for extreme braking conditions such as braking on split-μ surface or braking while cornering on slippery surface. Maximizing recuperated energy and preserving vehicle stability are thus conflicting objectives. A model predictive controller is proposed to coordinate the relationship between the regenerative braking system and the friction brakes in order to find the optimal compromise. The control objective is to maximize the regenerative braking while delivering the requested braking force, preserving stability and satisfying all system constraints. The suggested approaches prove to adequately balance the regenerative and friction braking forces so as to fulfil the control objective.

Keywords: Model Predictive Control, Optimal Control, Vehicle Dynamics Control, Electric Vehicle, Regenerative Braking, Vehicle Stability

Aknowledgements

I would like to thank my supervisor Paolo Falcone for his guidance during this project. Special thanks go to Mathias Lidberg Assistant Professor at the Division of Vehicle Engineering and Autonomous Systems for his many brilliant ideas, brainstorming, guidance on vehicle dynamics and his exceptional interest in the project. I thank my classmate Ehsan Harati for his help with the toolbox and other Matlab problems during the project's kick off period.
I would like to thank my family for their support throughout good and bad times during my University years. I thank my friends in Gothenburg for the good times and for being my family away from home. Of course, I thank my good friends back in Iceland for always being there for me. Lastly, I would like to thank my boyfriend Ragnar Lárusson for his love and support and for always knowing how to make me laugh.

Jóna Marín Ólafsdóttir

Göteborg October 2011
Jóna Marín Ólafsdóttir

Contents

Chapter 1

Introduction

Most electric vehicles today are equipped with a regenerative braking system. With regenerative braking the electric motor becomes a generator and transforms kinetic energy, that would otherwise be wasted as heat, into electric energy that is stored away in electricity buffers. Maximizing the energy recovery can therefore extend the driving range of the electric vehicle considerably.
Commonly the electric motor is present at the front axle. Maximizing regenerative braking and thus delivering most of the requested braking at a single axle can impose instability concerns on the vehicle. If the vehicle becomes unstable, stability controllers will be triggered and regenerative braking will be shut off. To prevent the repeated deactivation of energy recuperation an integrated controller is needed to divide the requested braking appropriately between friction and regenerative braking. The controller should maximize the energy recuperated while preserving vehicle stability, fully delivering the requested braking and satisfying all system constraints.
A Model Predictive Control (MPC) approach is used to control the yaw dynamics of the vehicle with the objective of fulfilling the state requirements. MPC is particularly useful for these purposes as it finds the optimal control sequence that minimizes a cost function subject to a set of constraints. Regenerative braking can thus effectively be maximized while design and system constraints are satisfied.

1.1 Scope

This work focuses on optimal state feedback control, more precisely model predictive control. It is assumed that the state measurements, yaw rate and longitudinal and lateral velocities, are readily available to the controller. In this case a Vehicle State Estimator (VSE) estimates the state measurements. The VSE is provided with signals from sensors on the vehicle and then uses a prediction model and an Extended Kalman Filter to estimate the states. The VSE used in this project was developed and provided by TNO, Netherlands. The vehicle simulation model was developed at the Division of Vehicle Engineering and Autonomous Systems at Chalmers University of Technology. For further information on the VSE and the vehicle simulation model refer to [1] and [2] respectively.
All actuator limitations and system bounds such as minimum/maximum braking torque of motor, minimum/maximum braking change rate, minimum/maximum allowable yaw rate have been roughly approximated. These values can easily be set to the true value of a real physical system.

Two types of controllers that use different brake blending techniques for the friction braking system were investigated; differential braking and variable braking balance between the front and rear axles. The performance of the two controllers were studied for two driving scenarios; braking during cornering on slippery surface and braking going straight on split-μ surface. All modelling and simulations presented in this thesis were carried out in Matlab/Simulink.

1.2 Contribution

The major contributions included in the research of this thesis work can be summarized as:

- Provides a general framework based on constrained optimal control approaches.
- Proposes a controller that successfully balances conflicting objectives. The controller maximizes regenerative braking, fully delivers the requested braking, prevents vehicle yaw instability, prevents wheel lock up and accounts for actuator limitations.
- Shows how the stated control problem can effectively be formulated and solved as an MPC problem.
- Validates the proposed approaches through simulation of different manoeuvre scenarios.
- Provides a good starting point for implementation on an actual vehicle.

1.3 Overview

Chapter 2 covers a brief overview of the history of electric vehicle's, the basics of regenerative braking and various control strategies for regenerative braking systems. The fundamentals of model predictive control are described in Chapter 3. The prediction model utilized by the MPC scheme is given in Chapter 4 and the proposed controller formulation is stated in Chapter 5. Simulation results are presented in Chapter 6 and Chapter 7 gives the concluding remarks.

Chapter 2

Electric Vehicles and Regenerative Braking

Electric vehicles were first introduced in the 19th century. In the late 19th century electric vehicles were a common way of passenger transportation in the US, Britain and France but they were soon to be replaced by the rapidly developing gasoline vehicle. Electric vehicles again became attractive however in the late 20th century when the contribution of transportation systems based on fossil fuels to global warming was realized and the sustainability of such systems became questionable. Electric vehicles emit no greenhouse gases and can be powered by the means of energy from renewable sources. Furthermore, they are equipped with regenerative braking systems that allow for the partial recuperation of kinetic energy, which would normally be wasted in a standard gasoline vehicle.

In order to fully deliver all of the braking force requested by the driver electric vehicles are also equipped with a conventional friction braking system. Coordinating the friction and regenerative braking with the objective of maximizing the recuperated energy can be a challenging control problem. This is especially true when the vehicle travels on slippery surface.

2.1 History of Electric Vehicles [3,4]

The invention of electric vehicles (EV) dates back to as far as 1834. The first electric automobile was later built in 1881 when improved battery technology was available. It was a 0.1 hp tricycle weighting 160 kg including its driver. In the following decades a number of EV designs were introduced including the first commercial EV. It was a taxi with two 1.5 hp motors and had a range of 40 km. During these years the first EV to reach a speed of 100 km/h was also built and by 1900, American car companies had made 1575 electric cars as opposed to 936 gasoline cars.
At this point the first hybrid electric vehicle (HEV) had also been invented, where electric motors were utilized to provide additional power to an internal combustion engine (ICE). In the early years of the 20th century thousands of EVs and HEVs were produced. Nevertheless, due to the rapid development of gasoline automobile technology, the discovery of large reserves of petroleum and the limitations associated with the batteries and high cost of EVs and HEVs their popularity and compatibility started to decline. By 1930 gasoline vehicles were completely dominating the automotive-market and EVs and HEVs vanished from the scene.

In the 1970s first the EV and then later the HEV started gaining interest again as both energy crisis and concerns about the environment compelled countries to seek alternative solutions to conventional ICE vehicles. Finally in 1997 the first modern commercialized HEV, the Toyota Prius, was released in Japan. The Prius can be considered as the first respond to the problem of passenger vehicle fuel consumption. Even though EVs take this respond even further with its zero emission, they still remain unavailable to the general public mainly by reason of high price and short range compared to conventional vehicles and lack of infrastructure.

2.2 Regenerative Braking

A very important feature of EVs and HEVs and one of their most significant technical advances is the regenerative braking system, introduced in late 19th century [4]. Regenerative braking is a process where the electric motor operates as a generator and converts the kinetic energy of the vehicle into electrical energy during braking. The electrical energy stored in the vehicle's batteries or ultra-capacitors, can later be used for propulsion and thereby extend the driving range considerably without any pollutant emission. By utilizing regenerative braking technology to recover energy that is generally wasted as heat with conventional friction braking systems, an electric vehicle's range can be extended by 8-25% [5]. This is particularly true in urban driving characterized by a stop-and-go pattern.
It should be noted that the amount of energy recovered depends not only on how much energy is available for dissipation but on the battery's state of charge (SOC) and its recharge rate. If the battery is already full at a braking instant and no electrical component is drawing power, regenerative braking cannot take place.
Under extreme braking situations like, e.g., emergency braking, the battery might not be able to recharge at a sufficiently high rate. Furthermore, the maximum braking torque that can be provided by the traction motor is limited and can therefore be lower than the braking torque requested by the driver in sudden stops at high speeds. Additional friction braking is thus necessary to fully provide the requested braking demand. Moreover, the friction braking is also needed to bring the vehicle to a complete halt, as the motor cannot generate electricity at very low speeds. In conclusion, the regenerative braking, for several reasons, always has to be blended with friction braking.

2.3 Various Control Strategies for Regenerative Braking Systems

As observed in Section 2.2, regenerative braking system and friction braking system need to coexist in EVs in order to fully deliver the braking functions demanded by the driver. The regenerative braking system, which in EVs is usually only present at the driven axle [4], needs to be controlled electronically. An obvious and straightforward control objective is to maximize the kinetic energy recovered by the regenerative braking system during braking. Clearly, this objective has to be achieved while delivering all of the demanded braking and preserving vehicle stability. Managing the relationship between the friction and regenerative braking can thus be a challenging control problem.

Various control strategies have been developed to coordinate the regenerative and fric-

tion braking systems. These can roughly be divided into two categories: series and parallel braking systems.

2.3.1 Parallel Braking System

In a parallel braking system the regenerative and friction braking occur in conjunction, i.e., in parallel. The conventional friction braking system has a predefined ratio of braking force distribution between the front and rear axle and the regenerative braking system adds additional braking force to the axle it is applied to. This setup allows for regenerative braking system to be added onto a vehicle that is equipped only with a conventional braking system. As the distribution of friction braking forces is fixed the parallel braking system does not require an integrated controller. The electric motor is controlled based on measurements from a pressure sensor in the hydraulic unit or a position sensor in the braking pedal. This makes it relatively simple to implement a parallel braking system compared to a series system. However, a parallel system does not have the same potential to recuperate energy [4,6].

2.3.2 Series Braking System

In a series braking system integrated control is exploited to manipulate the regenerative and friction braking distribution in an optimal way. With an integrated controller the series setup supports independent friction braking commands at each wheel. Furthermore, braking can be delivered solely by the regenerative braking system as long as the demanded braking is less than or equal to the maximum braking torque the electric motor can produce and the road adhesion allows for. If the requested braking exceeds the limitations of the electric motor the additional braking torque is delivered by the friction braking system. It should be noted that if the vehicle's stability is compromised during braking, friction braking must be commanded in order to keep the vehicle stable and still deliver the demanded braking. This is particularly true for cornering situations.
With an optimal distribution of the braking forces and the possibility of including the additional degrees of freedom, series systems generally have the ability to recover more energy than parallel systems. Also, better brake blending gives the driver an improved perception of the pedal feel.

Series Based Regenerative Braking Control Strategies in the Literature

The distribution strategy of the braking forces between the front and rear axle is of particular importance. It should always ensure vehicle safety and stability. Different algorithms to blend regenerative and friction braking have been proposed in the literature. Often these are based on the Ideal Braking Force Distribution (IBFD) curve. Following the distribution of the IBFD curve guarantees that the front and rear wheels will lock simultaneously when the braking forces reach the limit that the tire-ground adhesive can support. Normally these control algorithms aim to keep the front and rear axle braking ratio at or below the IBFD curve as reaching beyond it would cause the rear wheels to lock before the front wheels. Locking the rear wheels first would affect the directional stability of the vehicle [4].
In [6] the authors predefine a specific area under the IBFD curve that restricts the allowable front to rear braking ratio. To maximize the regenerative braking at the front axle, the

proposed controller sets the motor braking torque to be the smallest of the required braking torque, the braking torque limit of the front axle and the available braking torque of the motor. The friction braking provides the additional torque needed to keep the braking distribution within the predefined area and to deliver any additional braking forces that the motor cannot handle. A similar strategy is proposed in [4].
In [7] the authors propose an $\mathcal{L}_2$ optimal control for rear axle regenerative braking. The controller should maintain vehicle stability while minimizing the impact of disturbances on the regenerative braking. This is done by minimizing the $\mathcal{L}_2$ gain from the rear load disturbance, i.e., the commanded braking forces applied at the rear, to the longitudinal slip. This in turn minimizes the influence of lateral disturbance on the amount of recovered energy.

In this thesis a series based system is proposed. It is a model predictive optimal control strategy that uses a plant model to find the optimal control inputs based on the plant's behaviour over a predefined prediction horizon. Two control setups will be tested, one that distributes braking forces optimally between the two axles and a second that distributes braking forces optimally between the four wheels.

Chapter 3

Model Predictive Control

Model Predictive Control (MPC) is an advanced control methodology that uses a plant model to predict future outputs of the plant in order to plan an optimal future trajectory of control signals. Based on the current state of the plant a cost function is optimized, subject to a set of constraints. The solution of the optimization problem is a sequence of optimal control signals over a future finite time (prediction) horizon. The cost function can be designed to penalize deviations of the predicted outputs from a reference trajectory. In concurrence with the receding horizon principle, one of the central ideas of the MPC methodology [8], at each time step only the first of the optimal signals of the optimal future input trajectory is applied to the plant. The next sampling time interval the optimization problem is again formulated and solved over a shifted time horizon to obtain the next control move, see Figure 3.0.1.

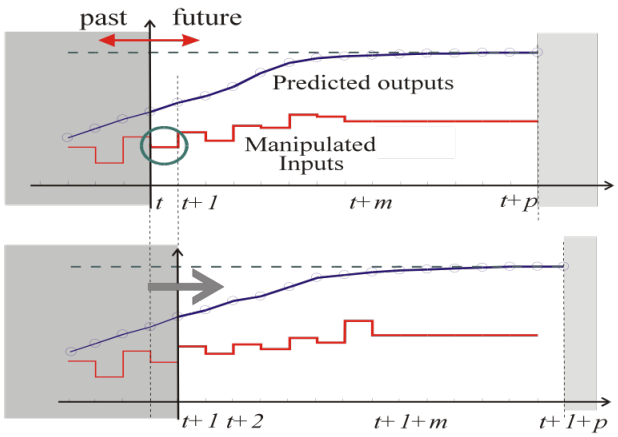

Figure 3.0.1: *Illustration of the receding horizon scheme.*

MPC was introduced during the 1960's. The MPC's biggest advantage over existing control techniques at that time, and still today, was its ability to handle constraints on inputs, outputs and states of plants and thereby take system limitations into account. This allowed for operating a system closer to the input and state space boundaries, a property that could be exploited to enhance profitability particularly within the chemical process industry [8]. By the late 1970's MPC was being widely used within the process industry. In recent years, with growing potential of computers and more extensive academic research, MPC has been applied to systems with harder real time restrictions such as applications

within the automotive industry [9].

In this chapter the basic MPC formulation for a nonlinear system is presented. For a nonlinear system the optimization problem will be subjected to nonlinear constraints. An optimization routine of a nonlinear optimization problem is bound to be computationally heavy, especially for higher order systems and long prediction horizons. An alternative formulation that can relax the computational burden is thus presented, a linear time varying case of the MPC whereas a nonlinear system can be approximated as a linear time varying system.

3.1 Nonlinear Model Predictive Control

Consider the discrete-time nonlinear system

$$x(k+1) = f(x(k), u(k)) \tag{3.1.1a}$$
$$y(k) = h(x(k), u(k)) \tag{3.1.1b}$$

where x is an n-dimensional state vector, u is an m-dimensional input vector and y is a p-dimensional vector of outputs which are to be controlled. The cost function J is defined as

$$J(x(k), U(k)) = \sum_{i=k}^{k+H_p-1} l(x(i), u(i)) \tag{3.1.2}$$

where l is the stage cost, $H_p \in \mathbb{Z}^+$ is the prediction horizon and $U(k) = [u(k), \ldots, u(k+H_p-1)]$. A control horizon can also be specified, H_u where $H_u \leq H_p$. The control sequence is therefore only calculated for H_u time steps and kept constant after that up to time $H_p - 1$, that is $u(k+i) = u(k+H_u-1)$, $i = H_u, \ldots, H_p - 1$.

To obtain the optimal control sequence $U_k^* = [u_{k,k}^*, \ldots, u_{k+H_p-1,k}^*]$ the following open-loop optimization problem is solved

$$\min_{U_k, x_{k+1,k}, \ldots, x_{k+H_p,k}} \quad J_{H_p}(x_k, U_k) \tag{3.1.3a}$$
$$\textit{subj. to} \quad x_{i+1,k} = f(x_{i,k}, u_{i,k}) \tag{3.1.3b}$$
$$y_{i,k} = h(x_{i,k}, u_{i,k}), \quad i = k, \ldots, k+H_p-1 \tag{3.1.3c}$$
$$x_{i,k} \in \mathcal{X}, \quad i = k, \ldots, k+H_p \tag{3.1.3d}$$
$$y_{i,k} \in \mathcal{Y}, \quad i = k, \ldots, k+H_p-1 \tag{3.1.3e}$$
$$u_{i,k} \in \mathcal{U} \tag{3.1.3f}$$
$$x_{k,k} = x(k) \tag{3.1.3g}$$

where $\mathcal{X}$, $\mathcal{Y}$ and $\mathcal{U}$ are sets of admissible states, outputs and control inputs, respectively. By applying U_k^* to the system (3.1.3b) the optimal state trajectory $x_{i,k}^*$ for $i = k+1, \ldots, k+H_p$ is obtained. Now according to receding horizon policy at time step k only the first control signal $u_{k,k}^*$ is applied to the plant while the rest of the control sequence is discarded. The plant evolves to the state $x(k+1) = x_{k+1,k}^*$ that is assumed to be measurable and is used to formulate and solve the optimization problem (3.1.3) again at time step $k+1$ over a shifted horizon.

Problem (3.1.3), referred to as Non-Linear Model Predictive Control problem (NL MPC), is in general a non-convex optimization problem as the prediction model (3.1.3b) often displays nonlinear behaviour. Solving a non-convex problem can demand high computational efforts. The NL MPC can therefore have prohibitive complexity for many real time applications. By approximating system (3.1.1) with a linear model, the computational complexity of the optimization problem can be reduced. An approximated MPC scheme based on successive linearizations is therefore presented next.

3.2 Linear Time Varying Model Predictive Control

System (3.1.1) can be approximated as the following Linear Time Varying (LTV) system

$$x(k+1) = A_{k,k}x(k) + B_{k,k}u(k) + d_{k,k} \tag{3.2.1a}$$
$$y(k) = C_{k,k}x(k) + D_{k,k}u(k) + e_{k,k} \tag{3.2.1b}$$

where $A_{k,k}$, $B_{k,k}$, $C_{k,k}$ and $D_{k,k}$ are the Jacobians of $f(x(k), u(k))$ and $h(x(k), u(k))$ evaluated at $[\overline{x}(k),\overline{u}(k)]$ where $[\overline{x}(k),\overline{u}(k)]$ is a nominal solution of the system (3.1.1) around which it is linearized. $A_{k,k}$, $B_{k,k}$, $C_{k,k}$, $D_{k,k}$, $d_{k,k}$ and $e_{k,k}$ are thus defined as

$$A_{k,k} = \left.\frac{\partial f}{\partial x}\right|_{\overline{x}_{k,k},\overline{u}_{k,k}} \tag{3.2.2a}$$
$$B_{k,k} = \left.\frac{\partial f}{\partial u}\right|_{\overline{x}_{k,k},\overline{u}_{k,k}} \tag{3.2.2b}$$
$$C_{k,k} = \left.\frac{\partial h}{\partial x}\right|_{\overline{x}_{k,k},\overline{u}_{k,k}} \tag{3.2.2c}$$
$$D_{k,k} = \left.\frac{\partial h}{\partial u}\right|_{\overline{x}_{k,k},\overline{u}_{k,k}} \tag{3.2.2d}$$
$$d_{k,k} = \overline{x}_{k+1,k} - A_{k,k}\overline{x}_{k,k} - B_{k,k}\overline{u}_{k,k} \tag{3.2.2e}$$
$$e_{k,k} = \overline{x}_{k+1,k} - C_{k,k}\overline{x}_{k,k} - D_{k,k}\overline{u}_{k,k} \tag{3.2.2f}$$

Considering the cost function (3.1.2) the optimization problem becomes

$$\min_{U_k, x_{k+1,k}, \dots, x_{k+H_p,k}} \quad J_{H_p}(x_k, U_k) \tag{3.2.3a}$$
$$\textit{subj. to} \quad x_{i+1,k} = A_{i,k}x_{i,k} + B_{i,k}u_{i,k} + d_{i,k}, \quad i = k, \dots, k+H_p-1 \tag{3.2.3b}$$
$$y_{i,k} = C_{i,k}x_{i,k} + D_{i,k}u_{i,k} + e_{i,k} \tag{3.2.3c}$$
$$x_{i,k} \in \mathcal{X}, \quad i = k, \dots, k+H_p \tag{3.2.3d}$$
$$y_{i,k} \in \mathcal{Y}, \quad i = k, \dots, k+H_p-1 \tag{3.2.3e}$$
$$u_{i,k} \in \mathcal{U} \tag{3.2.3f}$$
$$x_{k,k} = x(k) \tag{3.2.3g}$$

Again U_k^* is acquired and $u_{k,k}^*$ applied to the system to obtain $x(k+1)$ and solve problem (3.2.3) over a shifted horizon.

By realizing the plant as the linear constraints (3.2.3b) and (3.2.3c) and assuming that the cost function (3.1.2) is a quadratic function the optimization problem now becomes convex.

Chapter 4

Prediction Model

The optimization problem formulation described in Chapter 3 includes a model of the plant which is utilized to predict future outputs. This model, hereafter referred to as the *prediciton model*, is a mathematical representation of the system and describes its dynamical behaviour when excited with an external input signal. In this chapter a prediction model of a vehicle is described. The basic equations of motion describing the dynamics of the vehicle are stated. These include lateral, longitudinal and yaw motion.

In this work the notations $\star$ and $\bullet$ are adopted to distinguish between variables associated with the front and rear axles of the vehicle, i.e. $\star \in f, r$, and the left and right sides, $\bullet \in l, r$. Furthermore, the subscripts *f,l; f,r; r,l; r,r* stand for front-left, front-right, rear-left and rear-right, respectively.

4.1 Nonlinear Vehicle Model

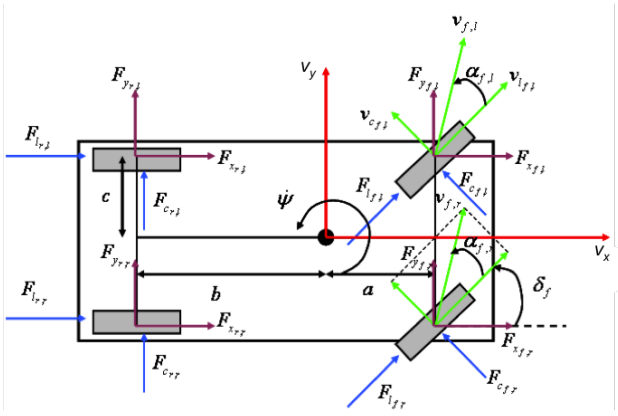

Figure 4.1.1: *Schematic figure of the vehicle dynamics. Black dot represents the vehicle's center of gravity, δ_f is the steering angle and $\alpha_{f,\bullet}$ are the slip angles [1].*

The simplified dynamics of a vehicle are illustrated in Figure 4.1.1. Assuming a rigid body, Newton's second law of motion gives the following set of differential equations describing the lateral, longitudinal and yaw dynamics

$$m\dot{v}_y = -mv_x\dot{\psi} + F_{y_{f,l}} + F_{y_{f,r}} + F_{y_{r,l}} + F_{y_{r,r}} \tag{4.1.1a}$$
$$m\dot{v}_x = mv_y\dot{\psi} + F_{x_{f,l}} + F_{x_{f,r}} + F_{x_{r,l}} + F_{x_{r,r}} \tag{4.1.1b}$$
$$\begin{aligned} I\ddot{\psi} = {} & a(F_{y_{f,l}} + F_{y_{f,r}}) - b(F_{y_{r,l}} + F_{y_{r,r}}) \\ & + c(-F_{x_{f,l}} + F_{x_{f,r}} - F_{x_{r,l}} + F_{x_{r,r}}) \end{aligned} \tag{4.1.1c}$$

where v_y is the lateral velocity, v_x is the longitudinal velocity and $\dot{\psi}$ the yaw rate. F_x and F_y are respectively the longitudinal and lateral tire forces in the vehicle's frame of reference, m the vehicle's mass and I its inertia. The parameters a, b and c are the dimensions as depicted in Figure 4.1.1. The mapping between tire forces in the vehicle and tire frame is

$$F_{y_{\star,\bullet}} = F_{l_{\star,\bullet}} \sin\delta_\star + F_{c_{\star,\bullet}} \cos\delta_\star \tag{4.1.2a}$$
$$F_{x_{\star,\bullet}} = F_{l_{\star,\bullet}} \cos\delta_\star - F_{c_{\star,\bullet}} \sin\delta_\star \tag{4.1.2b}$$

where F_l and F_c are the longitudinal and lateral tire forces in the tire frame, respectively. These forces are complex nonlinear functions of surface friction coefficient, the tire normal forces, slip ratios and slip angles [10]. The modeling of these forces will be described in Section 4.2.

4.2 Tire Force Modeling

The dynamics of a vehicle are highly influenced by the forces exerted by the road on each tire. Adequate modeling of the tire forces increases the strength of the prediction model. In this work the longitudinal forces are assumed to be equal to the braking forces, F_b, exerted on each tire

$$F_{l_{f,\bullet}} = F_{b_{f,\bullet}} = F_{f_{f,\bullet}} + \frac{1}{2}F_{RB} \tag{4.2.1a}$$
$$F_{l_{r,\bullet}} = F_{b_{r,\bullet}} = F_{f_{r,\bullet}} \tag{4.2.1b}$$

Here F_f denotes friction braking forces, i.e., forces generated by the friction braking system and F_{RB} are the forces generated by the regenerative braking system. Note that the regenerative braking forces are split equally between the front right and left wheels.

The lateral forces are complex nonlinear functions of several factors

$$F_{c_{\star,\bullet}} = f(\alpha_{\star,\bullet}, \mu_{\star,\bullet}, F_{l_{\star,\bullet}}, F_{z_{\star,\bullet}}) \tag{4.2.2}$$

where $\alpha_{\star,\bullet}$ are the slip angles, $\mu_{\star,\bullet}$ are the road friction coefficients, $F_{l_{\star,\bullet}}$ are the longitudinal forces and $F_{z_{\star,\bullet}}$ are the vertical forces. However, variation of the slip angle is commonly considered to be the most significant factor affecting the lateral force [11]. By exploring this dependency for a pure cornering manoeuvre (slip ratio $s = 0$) a linear relationship between

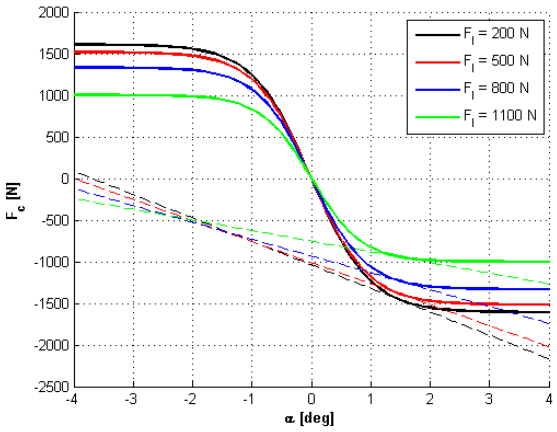

Figure 4.2.1: *Lateral force as a function of slip angle for* $\mu = 0.3$. *The dotted lines show the linearization at* $\alpha = 1.5°$.

the two variables can be detected within a certain interval, see Figure 4.2.1. Assuming that the vehicle operates mostly within the linear region lateral tire forces can be approximated as a linear function of the slip angles

$$F_{c_{\star,\bullet}} = -C_{c_{\star,\bullet}} \alpha_{\star,\bullet} \tag{4.2.3}$$

where C_c is the lateral stiffness coefficient, $C_c > 0$. Assuming C_c in (4.2.3) as constant can be a crude estimation however especially if the vehicle does in fact operate with slip angles that exceed $\pm 1°$. In order to model equation (4.2.3) more accurately a representation of the saturation effect at $\alpha > 1°$ and $\alpha < -1°$ is included. An analytical first order Taylor expansion of (4.2.2) is utilized to determine the approximate cornering stiffness at each time step depending on the current operating point.

The slip angle α is the angle between the corresponding wheel velocity vector and the wheel's actual direction

$$\alpha_{\star,\bullet} = \arctan \frac{v_{c_{\star,\bullet}}}{v_{l_{\star,\bullet}}} \tag{4.2.4}$$

where v_c and v_l are the lateral and longitudinal wheel velocities in the tire frame respectively, calculated as

$$v_{c_{\star,\bullet}} = v_{y_{\star,\bullet}} \cos\delta_\star - v_{x_{\star,\bullet}} \sin\delta_\star \tag{4.2.5a}$$
$$v_{l_{\star,\bullet}} = v_{y_{\star,\bullet}} \sin\delta_\star + v_{x_{\star,\bullet}} \cos\delta_\star \tag{4.2.5b}$$

with

$$v_{y_{f,\bullet}} = v_y + a\dot{\psi} \tag{4.2.6a}$$
$$v_{y_{r,\bullet}} = v_y - a\dot{\psi} \tag{4.2.6b}$$
$$v_{x_{\star,r}} = v_x + c\dot{\psi} \tag{4.2.6c}$$
$$v_{x_{\star,l}} = v_x - c\dot{\psi} \tag{4.2.6d}$$

where $v_{y_{\star,\bullet}}$ and $v_{x_{\star,\bullet}}$ are the lateral and longitudinal wheel velocities in the vehicle frame.

When considering combined cornering and braking manoeuvres equation (4.2.3) can be modified to include the interaction between longitudinal and lateral forces. Figure 4.2.2 shows this relationship for various slip angles α. A linear approximation can be used to model the nonlinear relationship between the longitudinal and lateral forces. Equation (4.2.3) thus now becomes

$$F_{c_{\star,\bullet}} = -C_{c_{\star,\bullet}}\alpha_{\star,\bullet} + D_{c_{\star,\bullet}}F_{l_{\star,\bullet}} \tag{4.2.7}$$

Using the same procedure for estimating D_c as for the estimation of C_c the lateral forces can now be determined.

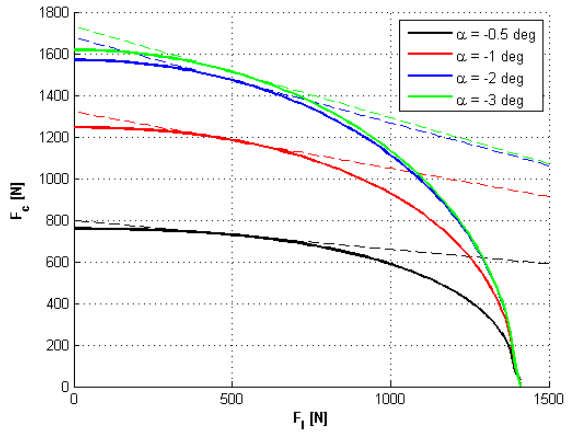

Figure 4.2.2: *Lateral force as a function of longitudinal force for* $\mu = 0.3$. *The dotted lines show the linearization at* $F_l = 500$ N.

4.3 Sate Space Formulation

The model (4.1.1) can be represented in the state space form

$$\dot{x}(t) = f(x(t), u(t), d(t)) \tag{4.3.1a}$$
$$y(t) = h(x(t)) \tag{4.3.1b}$$

where x denotes the state vector $x = \begin{bmatrix} v_y & v_x & \dot{\psi} \end{bmatrix}^T$, $d = [\delta_f]$ the disturbance and u is the input vector $u = \begin{bmatrix} F_{f_{f,l}} & F_{f_{f,r}} & F_{f_{r,l}} & F_{f_{r,r}} & F_{RB} \end{bmatrix}^T$. The output y of the prediction model is the vehicle's yaw rate, i.e., $y = \dot{\psi} = \begin{bmatrix} 0 & 0 & 1 \end{bmatrix} x(t)$. For a LTV MPC formulation model (4.3.1) can now be discretized and linearized according to (3.2.1a) and (3.2.2).

Chapter 5

Controller Formulation

When a driver issues a braking command while driving under harsh conditions such as cornering on a slippery surface, undesired yaw moment might be induced causing instability of the vehicle. Many vehicles today are equipped with a yaw stability control system that prevents yaw instability situations from arising. This system is activated as soon as the vehicle's yaw rate deviates excessively from a nominal behaviour. If this occurs during regenerative braking, the regenerative braking system will immediately be shut off as stability concerns are of higher priority than energy recuperation.
The main control objective of the regenerative braking control system is to maximize the amount of energy recovered. With the regenerative braking system placed at the driven axle, here the front axle, maximizing the energy recuperation implies that most of the braking should occur at the front axle. Concentrating braking forces mainly at one axle, particularly in a cornering manoeuvre on a slippery surface, can cause instability. Maximizing regenerative braking and preserving stability are thus two conflicting objectives that need to be compromised.
Vehicle instability initiates the activation of yaw stability systems and consequently the deactivation of the regenerative braking. The proposed controller should therefore include stability system activation criteria to facilitate the prevention of frequent deactivation of energy recuperation. Furthermore, the controller should always deliver all of the braking demanded by the driver.

The MPC framework has the option of including system constraints as a part of the optimization problem in a relatively simple manner. This is a highly beneficial property as many systems are subjected to physical limitations and/or are obligated to fulfil specific requirements. Constraints that are imposed on the system will be described in this chapter. Finally it is shown how the considered energy recuperation maximization problem can be effectively formulated and solved as an MPC problem.

5.1 Control Objective

The control objective can be stated as follows;

To maximize regenerative braking while preserving stability and satisfying the demanded braking.

The cost function in the optimization problem (3.2.3) should be defined with respect to

this objective. To preserve stability the cost function should include a term penalizing the yaw rate deviation from a desired yaw rate. Therefore the cost function is defined as

$$J(x(k), U(k), \Delta U(k)) = \sum_{i=0}^{H_p-1} \|y(k+i) - y_{ref}(k+i)\|_Q^2 + \sum_{i=0}^{H_u-1} \left[\|u(k+i)\|_S^2 + \|\Delta u(k+i)\|_R^2 \right] \tag{5.1.1}$$

where Q and S are positive semi-definite weighting matrices and R is a positive definite weighting matrix. The first term in the cost function penalizes deviations of the output, here yaw rate, from a reference trajectory. The second term allows for prioritization of the control signals, here braking forces, and thus maximization of the regenerative braking force. The third and last term penalizes the rate of change of braking and assures that the applied control efforts are smooth.
The control objective also states that the requested braking must be satisfied. This demand is not a part of the cost function but more exactly implemented as a system constraint (see Chapter 5.2).

5.2 Constraints

Considering the physical limitations of the braking actuators, i.e. friction brakes and the electric motor, boundaries can be defined on both the braking amplitude and rates. The amount of braking and its rate of change are therefore bounded as follows

$$u_{min_{i,k}} \leq u_{i,k} \leq u_{max_{i,k}} \tag{5.2.1}$$

$$\Delta u_{min_{i,k}} \leq \Delta u_{i,k} \leq \Delta u_{max_{i,k}} \tag{5.2.2}$$

$$i = k, ..., k + H_u - 1$$

The bounds can be either time varying or constant.

As mentioned in the control objective, the driver's braking demand must be fully delivered. Hence the demanded braking force, F_D, is a combination of friction and regenerative braking forces and the following equality should always hold

$$F_{D_{i,k}} = \left(F_{f_{f,l}} + F_{f_{f,r}} + F_{f_{r,l}} + F_{f_{r,r}} + F_{RB} \right)_{i,k} \tag{5.2.3}$$

$$i = k, ..., k + H_u - 1$$

The requested braking might exceed the friction forces that are available relative to the limitation of the adhesive between the ground surface and the tires. This can especially occur on slippery surfaces. To prevent the controller from demanding excessive braking forces they are bounded to an approximate maximum available force based on information about the surface friction coefficient μ and normal force F_z

$$(F_{l_{\star,\bullet}})_{i,k} \leq \left(\mu_{\star,\bullet} F_{z_{\star,\bullet}} \right)_{i,k} \tag{5.2.4}$$

$$i = k, ..., k + H_u - 1$$

Clearly, as long as the vehicle's battery is not full it is desirable to have the electric motor generate electricity at all possible times, i.e., at braking instants. Situations that may cause the regenerative braking system to be shut off by controllers with higher priority must therefore be avoided. These situations occur, e.g., when the vehicle's yaw rate deviates too much from a nominal behaviour, due to excessive braking delivered at a single axle. Reaching undesired yaw rate is discouraged through the first term of the cost function (5.1.1) by penalizing deviations from a reference yaw rate. However, this condition does not guarantee that the yaw rate will not deviate beyond a predefined threshold. Therefore a constraint is introduced that forces the yaw rate to stay within a certain interval. To avoid feasibility issues the constraint is relaxed (soft constrained), i.e., violations of the constraint are permitted but penalized. The constraint is formulated with respect to yaw rate error as follows

$$\dot{\psi}_{min_{i,k}} - \epsilon \leq \dot{\psi}_{i,k} - \dot{\psi}_{ref_{i,k}} \leq \dot{\psi}_{max_{i,k}} + \epsilon \qquad (5.2.5)$$
$$i = k, ..., k + H_c - 1$$

where $\epsilon \geq 0$ is a slack variable and H_c is the constraint horizon. The cost function (5.1.1) can now be modified to include the soft constraint

$$J(x(k), U(k), \Delta U(k), \epsilon) = \sum_{i=0}^{H_p-1} \|y(k+i) - y_{ref}(k+i)\|_Q^2 + \sum_{i=0}^{H_u-1} \left[\|u(k+i)\|_S^2 + \|\Delta u(k+i)\|_R^2 \right] + \rho\epsilon^2 \qquad (5.2.6)$$

5.3 Proposed Controller

By combining the prediction model described in Chapter 4, the cost function (5.2.6) and the constraints (5.2.1) to (5.2.5) the MPC problem for the regenerative braking control system can be formulated as

$$\min_{\Delta U_k, x_{k+1,k}, \ldots, x_{k+H_p,k}, \epsilon} \quad J_{H_p}(x_k, \Delta U_k, \epsilon) \qquad (5.3.1a)$$
$$subj.\ to \quad x_{i+1,k} = A_{i,k}x_{i,k} + B_{i,k}u_{i,k} + d_{i,k} \qquad (5.3.1b)$$
$$y_{i,k} = \begin{bmatrix} 0 & 0 & 1 \end{bmatrix} x_{i,k} = \dot{\psi}_{i,k} \qquad (5.3.1c)$$
$$i = k, \ldots, k + H_p - 1$$
$$constraints\ (5.2.1)\ to\ (5.2.5)$$

and

$$u^\star_{k,k} = u_{k-1,k} + \Delta u^\star_{k,k} \qquad (5.3.2)$$

where $\Delta u^\star_{k,k}$ is the first element of $\Delta U^\star_{k,k}$, sequence of optimal control moves, applied to system (5.3.1b) in receding horizon. Problem (5.3.1) can now be formulated and solved as a standard Quadratic Programming (QP) problem [8]

$$\min_{\theta_k} \ \frac{1}{2}\theta^T_{k,k}\Phi\theta_{k,k} + \varphi^T\theta_{k,k} + \beta \qquad (5.3.3a)$$
$$subj.\ to \quad \Omega\theta_{k,k} \leq \omega \qquad (5.3.3b)$$

where the matices Φ, φ and β are derived from the cost function (5.2.6), Ω and ω are derived from constraints (5.2.1) to (5.2.5) and θ is the augmented state vector $\theta = \begin{bmatrix} x_{k,k} & u_{k,k} \end{bmatrix}^T$.

Chapter 6

Results

To test the MPC formulation (5.3.1) two different controllers were designed and validated with simulation. One controller exploits differential brake blending and a second controller applies variable braking balance between the front and rear axles. The two controllers were tested for two different manoeuvre scenarios where in the first one the vehicle brakes during cornering on a slippery surface. In the second manoeuvre the vehicle brakes while going straight on a split-μ surface.

6.1 Controllers

Two types of controllers were simulated. The first controller, obtained by solving problem (5.3.1) and referred to as Controller i, allows for individual friction braking at each wheel. The second controller, Controller ii, equally splits the friction forces between the two wheels at each axle. Controller ii is derived from problem (5.3.1) with the additional constraints

$$F_{f_{f,l}} = F_{f_{f,r}} \tag{6.1.1a}$$
$$F_{f_{r,l}} = F_{f_{r,r}} \tag{6.1.1b}$$

The controller parameters for the two controllers are;

Sampling time: $T = 0.01$ s

Horizons: $H_p = 15$, $H_u = 3$, $H_c = 3$

Bounds:

u		Δu		$\dot{\psi}$	
LB	UB	LB	UB	LB	UB
0 N	3000 N	$-2 * 10^5$ N	$2 * 10^5$ N	$-2°$	$2°$

Weighting matrices:

$Q = 0$

$$S = \begin{bmatrix} 400 & 0 & 0 & 0 & 0 \\ 0 & 400 & 0 & 0 & 0 \\ 0 & 0 & 400 & 0 & 0 \\ 0 & 0 & 0 & 400 & 0 \\ 0 & 0 & 0 & 0 & 0 \end{bmatrix}$$

$$R = \begin{bmatrix} 10^4 & 0 & 0 & 0 & 0 \\ 0 & 10^4 & 0 & 0 & 0 \\ 0 & 0 & 10^4 & 0 & 0 \\ 0 & 0 & 0 & 10^4 & 0 \\ 0 & 0 & 0 & 0 & 10^2 \end{bmatrix}$$

$$\rho = 8 * 10^6$$

Note that the bounds on u and Δu should be set with respect to the specifications of the vehicle's motor and friction brakes. Bounds on $\dot{\psi}$ should be set to a value that is within the activation threshold of the vehicle's yaw stability controllers.

6.2 Simulation Scenarios

The controllers were tested for two different vehicle manoeuvres referred to as Manoeuvres 1 and 2. Table 6.2.1 summarizes Manoeuvres 1 and 2.

6.2.1 Manoeuvre 1

In Manoeuvre 1 the vehicle is cornering with a constant steering angle of 30° on a slippery surface when braking is issued after the vehicle's yaw rate reaches a steady state value. Figure 6.2.1(a) shows the steering wheel angle and the respective braking profile of Manoeuvre 1.
It is interesting to examine the vehicle's response for the given manoeuvre when all of the requested braking is delivered as regenerative braking. Figure 6.2.1(b) shows the yaw rate response for Manoeuvre 1. Keeping in mind that braking occurs between 10 – 13 s it is apparent that without the controller the yaw rate bounds are violated during braking. In this case higher priority stability controllers would have been activated and the regenerative braking simultaneously shut off.

6.2.2 Manoeuvre 2

In Manoeuvre 2 the vehicle is travelling straight on a slippery, split-μ surface when a braking command is issued. On a split-μ surface the left and right side of the vehicle are subjected to different surface friction coefficients. In the considered manoeuvre the left side of the road has higher friction road coefficient. Figure 6.2.2(a) shows the respective braking profile of Manoeuvre 2.
Figure 6.2.2(b) shows the commanded longitudinal forces when all of the requested braking is delivered as regenerative braking. It shows that for the front right tire longitudinal force

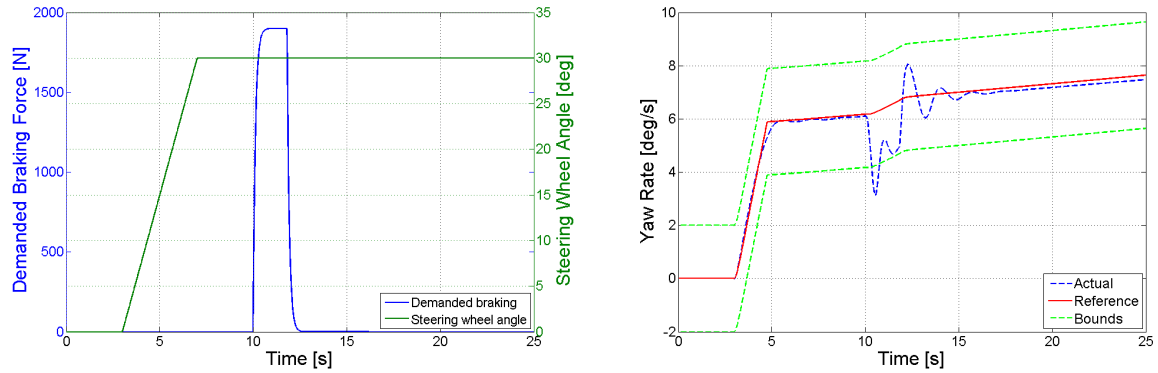

(a) *Braking profile and steering wheel angle.* (b) *Yaw rate response.*

Figure 6.2.1: *Manoeuvre1: Braking profile and steering wheel angle (left), yaw rate response when demanded braking is delivered through regenerative braking only (right).*

exceeds the maximum allowable force defined by constraint (5.2.4). This would cause the wheel to lock and trigger other stability controllers. Again no regenerative braking would occur during braking.

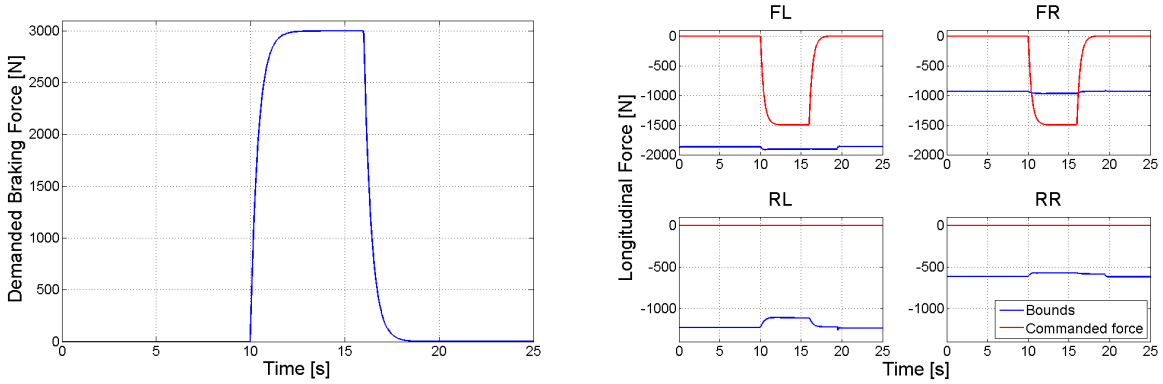

(a) *Braking profile.* (b) *Commanded and maximum longitudinal forces.*

Figure 6.2.2: *Manoeuvre 2: Braking profile (left), commanded longitudinal forces and maximum longitudinal forces (bounds) when demanded braking is delivered through regenerative braking only (right).*

Table 6.2.1: *Parameters for Manoeuvres 1 and 2*

	Manoeuvre 1	**Manoeuvre 2**
Initial velocity [km/h]	100	100
Steering wheel angle [deg]	30	0
Braking pulse [g]	0.12	0.18
Road friction coefficient	0.3	
Left		0.4
Right		0.2

6.3 Simulation Results

6.3.1 Manoeuvre 1

The results for the two controllers when the vehicle is in Manoeuvre 1 are depicted in Figure 6.3.1. The vehicle is turning to the left and starts braking after 10 s. Maximizing the regenerative braking causes most of the braking force to be delivered at the front axle. This decreases the vehicle's turning rate and the vehicle becomes understeered. To counteract for the understeering effect and keep the yaw rate within its bounds, friction braking is triggered in both controllers. With Controller i (Figure 6.3.1(a)) friction braking is initiated on three wheels, mostly on the front and rear left wheels. By inducing braking on the left side understeering is decreased and yaw rate bound violation is avoided. No friction braking is present at the front right wheel. With Controller i 90.91% of the demanded braking is delivered through regenerative braking.
Controller ii (Figure 6.3.1(b)) is restricted to brake equally on both wheels of each axle. As increasing the braking force on the front would cause the vehicle to understeer even more Controller ii uses only regenerative braking to brake on the front and counteracts for understeering by braking on the rear. With Controller ii 90.55% of the demanded braking is delivered through regenerative braking.

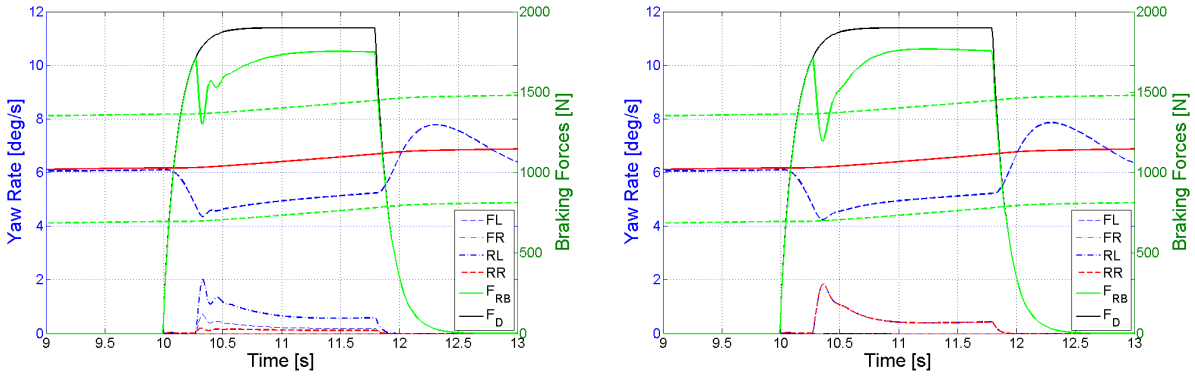

(a) *Controller i.* (b) *Controller ii.*

Figure 6.3.1: *Braking forces and yaw rate response (wide blue dashed line) for Manoeuvre 1. Red solid line represents the yaw rate reference and green dashed lines are the upper and lower yaw rate bounds.*

6.3.2 Manoeuvre 2

Figures 6.3.2 and 6.3.3 show the result for the two controllers when the vehicle is in Manoeuvre 2. The vehicle is travelling straight with a friction coefficient as low as 0.2 on the right side and 0.4 on the left side. With such low road friction the allowable braking forces will be limited for a high demanded braking force. This becomes apparent when looking at the longitudinal forces (braking forces) commanded by Controller i on Figure 6.3.2(b) where forces on the front right wheel clearly hit the bound of maximum allowable longitudinal force limited by the road friction. The road friction therefore limits the amount of achievable regenerative braking for this manoeuvre. The controller issues as much regenerative braking as constraint (5.2.4) for the front right wheel allows for, i.e. no

friction braking occurs at the front right wheel. To fulfil the demanded braking request the controller delivers the remaining braking with friction braking forces divided equally between the other three wheels (see Figure 6.3.2(a)). The achieved amount of regenerative braking is 69.07% of the demanded braking.
Similar behaviour is noticed for Controller ii (see Figure 6.3.3). The ground adhesive at the front right tire limits the amount of regenerative braking and no friction braking is issued at that tire. Friction forces are now split equally between the rear tires only to deliver the remainder of the demanded braking. With this strategy almost no yaw rate error is realized. The achieved amount of regenerative braking is 68.73% of the demanded braking.
Table 6.3.1 summarizes the achieved regenerative braking for the two controllers and manoeuvres.

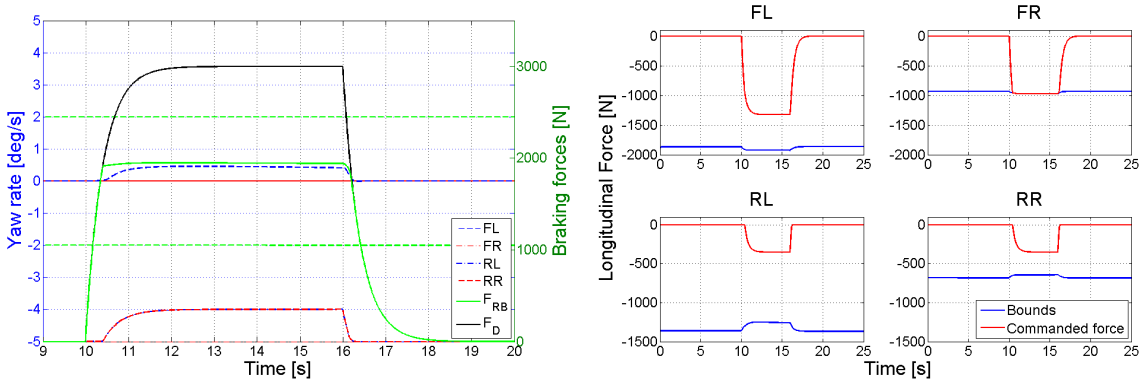

(a) *Braking forces and yaw rate response.*

(b) *Commanded and maximum longitudinal forces (bounds).*

Figure 6.3.2: *Simulation results for Controller i, Manoeuvre 2. On Figure (a) wide blue dashed line represents the yaw rate response, red solid line the yaw rate reference and green dashed lines the upper and lower yaw rate bounds.*

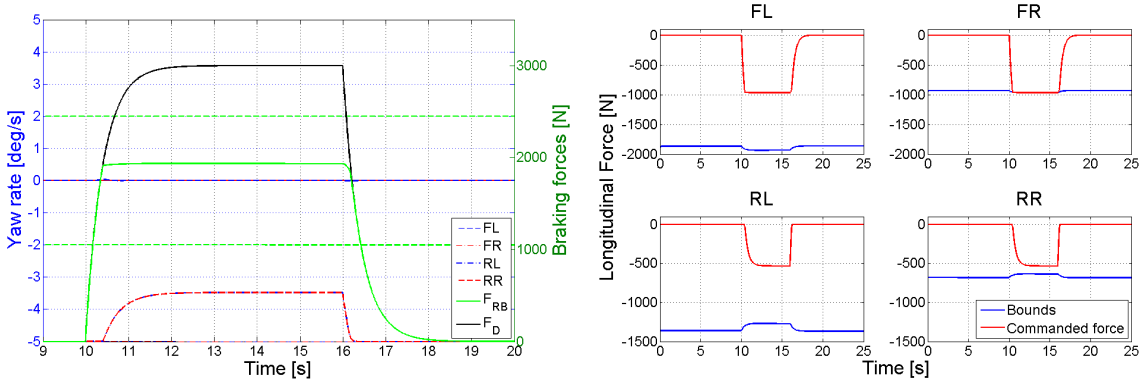

(a) *Braking forces and yaw rate response.*

(b) *Commanded and maximum longitudinal forces (bounds).*

Figure 6.3.3: *Simulation results for Controller ii, Manoeuvre 2. On Figure (a) wide blue dashed line represents the yaw rate response, red solid line the yaw rate reference and green dashed lines the upper and lower yaw rate bounds.*

Table 6.3.1: *Percentage of demanded braking delivered through regenerative braking for both controllers and manoeuvres.*

	Manoeuvre 1	**Manoeuvre 2**
Controller i	90.91%	69.07%
Controller ii	90.55%	68.73%

As can be noticed on Figure 6.3.3(b) the commanded forces at the rear right tire are close to hitting the bound of maximum allowable force as well. It is therefore interesting to investigate the controller's respond when the forces on the right side are completely saturated. For these purposes the friction coefficient on the right side is lowered from 0.2 to 0.18. Figure 6.3.4 shows the longitudinal forces commanded by Controller ii in such a manoeuvre. As Figure 6.3.4 shows, the forces on the right side are saturated and for the rear right tire the maximum allowable force bound is violated. Controller ii issues as much braking on the front axle as is permitted by the bound on the front right tire. Now when it tries to issue the rest of the demanded braking on the rear axle the command is interrupted by the bound on allowable forces at the rear right tire. Apparently, the controller cannot satisfy the constraint on the rear right tire or demanded braking and the solution becomes unfeasible.
Controller i however, succeeds to satisfy all constraints for this manoeuvre setup, see Figure 6.3.5. Exploiting its additional degrees of freedom, controller i delivers as much forces at the front axle as is permitted by the bound on the front right tire and splits as before the rest of the demanded braking equally between the other three wheels. The achieved regenerative braking was 62.87% of the requested braking.

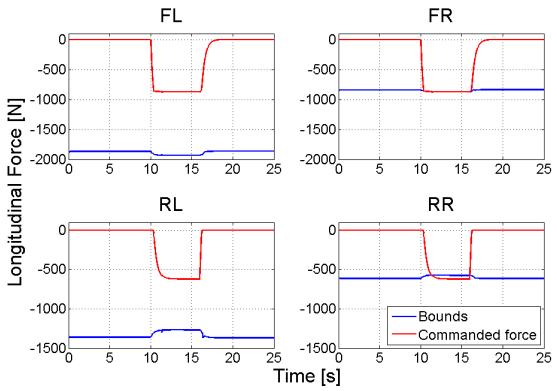

Figure 6.3.4: *Commanded longitudinal forces and maximum longitudinal forces (bounds) for Controller ii, Manoeuvre 2 with* $\mu = 0.18$ *on the right side.*

6.3.3 Braking Distribution

When a braking command is issued during driving, load is transferred from the rear to the front of the vehicle. To counteract this behaviour braking forces are distributed in such a way that the vehicle brakes harder in the front. Even though the load transfer depends highly on the deceleration, the distribution ratio generally has a predefined value. This value is commonly set to be 70/30, i.e., 70% of the braking forces are delivered at

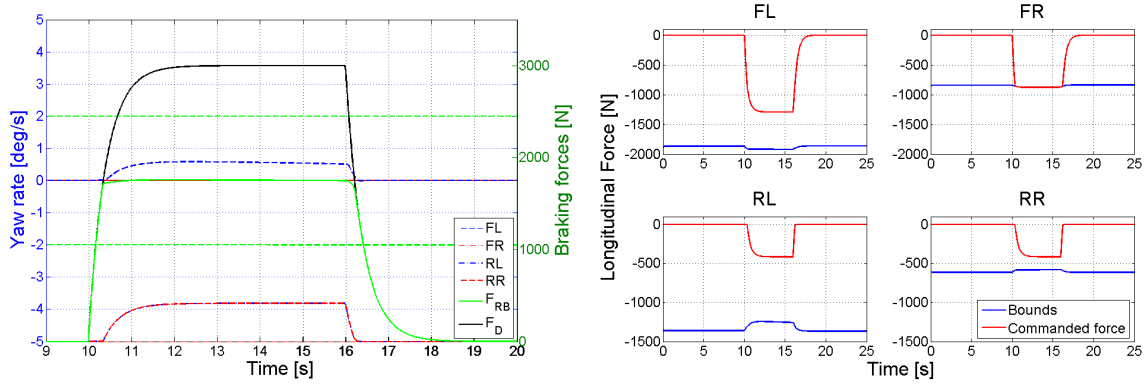

(a) *Braking forces and yaw rate response.*

(b) *Commanded and maximum longitudinal forces (bounds).*

Figure 6.3.5: *Simulation results for Controller i, Manoeuvre 2 with* $\mu = 0.18$ *on the right side. On Figure (a) wide blue dashed line represents the yaw rate response, red solid line the yaw rate reference and green dashed lines the upper and lower yaw rate bounds.*

the front and 30% at the rear. Fixing the distribution ratio to a specific value however can be too conservative, considering that vehicles do encounter various scenarios with different decelerations. It is therefore interesting to investigate how Controller ii, that has a variable distribution ratio, allocates the amount of braking between the two axles. Figure 6.3.6 shows the braking distribution for Manoeuvres 1 and 2. Figure 6.3.6(b) shows that for Manoeuvre 2, Controller ii distributes the forces quite close to the common 70/30 ratio or roughly 65/35 on average during most of the braking. For Manoeuvre 1 however (see Figure 6.3.6(a)) up to 93% of the braking is delivered at the front confirming that the 70/30 constraint is not ideal for such a braking manoeuvre and would in turn cause less energy to be recuperated.

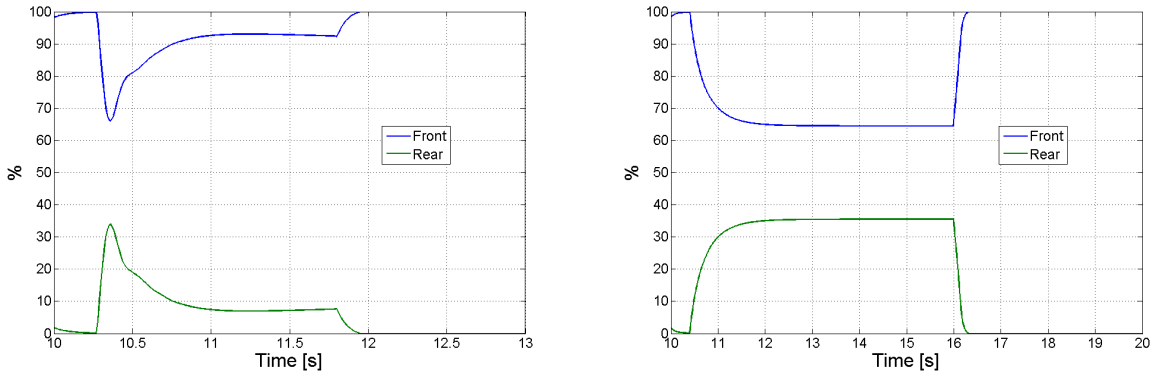

(a) *Manoeuvre 1.*

(b) *Manoeuvre 2.*

Figure 6.3.6: *Braking distribution of Controller ii.*

Chapter 7

Conclusions

The results presented in Section 6.3 show that both controllers succeed to fulfil the control objective in Manoeuvres 1 and 2. In all four cases yaw rate stays within its specified bounds during braking. Stability of the vehicle is preserved and activation of higher order stability controllers is avoided. Demands on requested braking and other constraints are satisfied in all four simulations. Maximum amount of 90.91% and 69.07% of the demanded braking was recuperated with controller i for manoeuvres 1 and 2 respectively. However the difference in recuperation percentage between the two controllers was less than 0.36% for both manoeuvres. The results from Manoeuvres 1 and 2 conclude that with respect to maximizing regenerative braking the two additional degrees of freedom of the differential braking setup do not provide a substantial improvement in performance for these particular manoeuvres. However, if the friction coefficient on the right side is decreased from 0.2 to 0.18 in Manoeuvre 2, it is observed that Controller ii cannot satisfy constraints both on maximum longitudinal forces and demanded braking. Conversely, Controller i succeeds to fulfil all constraints by utilizing its additional degrees of freedom. In conclusion, the additional degrees of freedom of Controller i can provide extended flexibility for extremely challenging manoeuvres.
The MPC approach has been shown to be a versatile method that can adapt to different controller setup and various braking manoeuvre configurations. It performs well in challenging situations such as the scenarios presented and with the suitable tuning parameters it adequately balances conflicting objectives. From this it can be inferred that the presented setup is a good starting point for implementation on an actual electric vehicle.

Bibliography

[1] P. Falcone, M. Lidberg, J. M. Ólafsdóttir, S. Jansen and S. van lersel. *Control and State Estimation for Energy Recuperation in Fully Electric Vehicles*. 20th Aachen Colloquium Automobile and Engine Technology, Oct. 2011.

[2] M. Lidberg, J. Alfredson. *Control of the Direction Sensitive Locking Differential (DSLD) for a Front Wheel Drive Passenger Car in Transient Cornering*. Proceedings of the IAVSD 2009 Conference, 2009.

[3] C. C. Chan. *The State of The Art of Electric, Hybrid, and Fuel Cell Vehicles*. Proceedings of the IEEE, vol. 95, No. 4, Apr. 2007.

[4] M. Ehsani, Y. Gao, S. E. Gay and A. Emadi. *Modern Electric, Hybrid Electric, and Fuel Cell Vehicles*. CRC Press LCC, Boca Raton, U.S., 2005.

[5] M. K. Yoong, Y. H. Gan, C. K. Leong, Z. Y. Phuan, B. K. Cheah, K. W. Chew. *Studies of Regenerative Braking in Electric Vehicle*. IEEE Conference on Sustainable Utilization and Development in Engineering and Technology, Nov. 2010.

[6] J. Guo, J. Wang and B. Cao. *Regenerative Braking Strategy for Electric Vehicles*. IEEE Intelligent Vehicles Symposium, Jun. 2009.

[7] S. Solyom, F. Bruzelius. $\mathcal{L}_2$ *Control of Regenerative Braking for Hybrid Electric Vehicles*.

[8] J. M. Maciejowski. *Predictive Control with Constraints*. Pearson Education Ltd., Harlow, England, 2002.

[9] E. F. Camacho and C. Bordons. *Model Predictive Control*. Springer, New York, U.S., 2004.

[10] R. Rajamani. *Vehicle Dynamics and Control*. Springer, New York, U.S., 2006.

[11] P. Falcone. *Nonlinear Model Predictive Control for Autonomous Vehicles*. Phd thesis, University of Sannio, Italy, 2007.